Geophys. J. Int. (2005) **161,** 1–11 doi: 10.1111/j.1365-246X.2005.02518.x

Lake level variations in China from TOPEX/Poseidon altimetry: data quality assessment and links to precipitation and ENSO

Cheinway Hwang,[1] Min-Fong Peng,[1] Jinsheng Ning,[2] Jia Luo[2] and Chung-Hsiung Sui[3]

[1] *Department of Civil Engineering, National Chiao Tung University,* 1001 *Ta Hsueh Road, Hsinchu* 300, *Taiwan. E-mail: hwang@geodesy.cv.nctu.edu.tw*
[2] *School of Geodesy and Geomatics, Wuhan University,* 129 *Luoyu Road, Wuhan* 430079, *China*
[3] *Institute of Hydrological Sciences, National Central University, Chungli, Taiwan*

Accepted 2004 October 26. Received 2004 October 25; in original form 2003 August 22

SUMMARY

About 10 yr of TOPEX/Poseidon (T/P) altimetry data have been used to compute time series of lake levels at six inland lakes in China. To verify our T/P data processing strategy, the T/P-derived lake levels at Bosten Lake (west China) and Lake Huron (north America) were compared with lake gauge records: good agreement is found between the T/P and the gauge results. Wavelet spectra indicate annual and interannual variations of these lake levels, which are also sensitive to climate variability. At the interannual timescale, the lake levels of Hulun (north China), Bosten (west China) and Ngangzi (east Tibet) are correlated with precipitation and El Niño Southern Oscillation (ENSO); in particular, they all respond to the 1997–1998 El Niño. The Bosten lake level has increased monotonically since 1993 due to the increased temperature on Tianshan Mountain, which feeds water into this lake. The lake levels of Hongze and Gaoyou (east China) show minor decreasing trends. The lake level of La'nga (west Tibet) decreased steadily from 1993 to 2001, with a total drop of 4 m. The Ngangzi lake level decreased from 1993 January to 1997 December, but after the peak of the 1997–1998 El Niño the slope was reversed and the lake level has increased monotonically since then. An example given at Bosten Lake shows that waveform contamination over Chinese lakes affects the quality of T/P-derived lake levels and retracking is necessary to mitigate the problem.

Key words: ENSO, lake level in China, Tibet, TOPEX/Poseidon.

1 INTRODUCTION

TOPEX/Poseidon (T/P) (see e.g. Fu *et al.* 1994) is a satellite altimetry mission primarily designed to measure sea-surface heights. However, T/P altimetry data have also been used to study inland lakes in the US (Morris & Gill 1994), Africa (Birkett 1995; Mercier *et al.* 2002), and South America (Alsdorf *et al.* 2001; Berry 2003). The results from these studies show that T/P can also measure the heights of inland lakes with a precision similar to that over the oceans. The results also show how some of the climatically sensitive lakes respond to climate change. In particular, Mercier *et al.* (2002) found that the interannual variations of lake levels in Africa are associated with the El Niño Southern Oscillation (ENSO). In fact, land application of satellite altimetry has become so important that the International Association of Geodesy (IAG) will establish a special study group (SSG) to explore the use of altimetry data over land (P. Berry & C. Jekeli, private communication, 2003).

There are also several large inland lakes in China, which are mainly distributed in east China, northeast China, Xinjiang, the Tibetan Plateau and in areas along the Yangtze River (Fig. 1). To see the performance of T/P over Chinese inland lakes and to see how the inland lakes respond to climate change, we will process T/P altimetry data to obtain time series of lake level for selected Chinese inland lakes. Relationships among lake levels in China, precipitation and ENSO will be investigated. In the search for an improved lake-level determination, the problem of waveform contamination of T/P data over inland lakes will be discussed.

2 THE CHINESE INLAND LAKES STUDIED

We select all lakes in China with T/P ground tracks passing through them and with reliable altimetry data. In total there are six such lakes (Fig. 2). Table 1 lists the appropriate T/P passes and selected features of these lakes. There is no T/P pass over Qinghai Lake, which is the largest salt-water lake in China, nor over Poyang and Dongting lakes, which are the largest and second-largest fresh-water lakes. In Table 1, 'regulation' means that the water volume is regulated as needed. Orbit manoeuvres of T/P are normally performed over land, where the precision of the T/P orbit, and hence the precision of the observed lake heights at and near the manoeuvring times, will be degraded. The continent of Eurasia is the largest landmass in the world, and thus orbit manoeuvres of T/P are very likely to occur here. Furthermore, Hulun, Bosten, La'nga and Ngangzi lakes

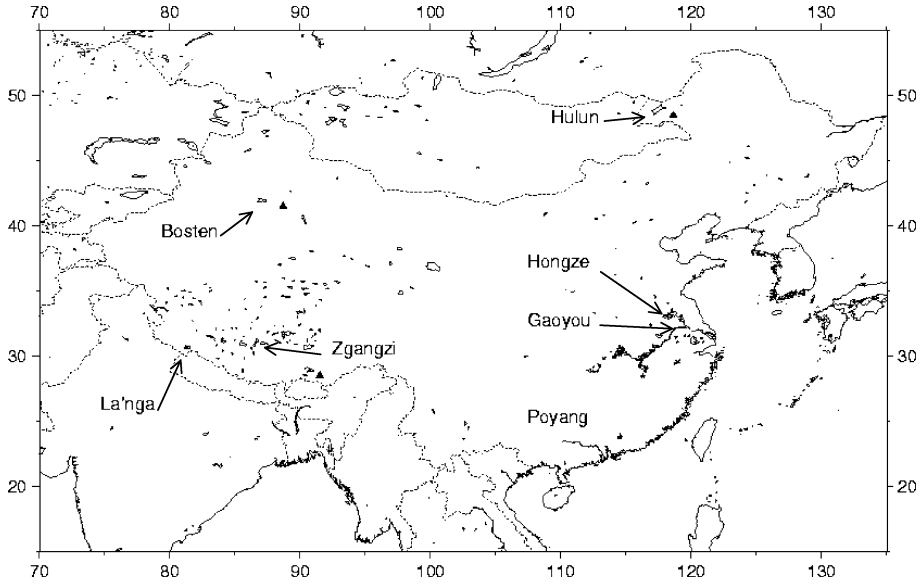

Figure 1. Locations of the six studied lakes in China. Triangles represent precipitation stations.

Table 1. Features of the six studied lakes in China.

Lake	Borders longitude latitude	Mean ellipsoidal height[1] (m)	Surface area (km^2)	T/P pass	No. of 1-Hz points	Regulated	Type
Hulun	117.875–118.875, 48.500–49.500	533.92	2315	36	3	no	open
Bosten	86.500–87.500, 41.500–42.500	985.81	1043	64	2	yes	open
La'nga	80.750–81.750, 30.250–31.250	4524.95	394	181	1	no	closed
Ngangzi	86.500–87.500, 30.500–31.500	4624.44	244	79	1	no	closed
Hongze	118.000–119.000, 32.750–33.750	13.10	2069	240	2	yes	open
Gaoyou	118.750–119.750, 32.250–33.250	7.79	775	153	3	yes	open

[1]Above the GRS80 ellipsoid with a semimajor axis of 6378136.3 m. Derived from T/P altimetry.

are located either at high latitude or at high altitude, and thus their surfaces will be covered with ice in winter. The lake heights derived from geophysical data records (GDRs) of Archivings Validation and Interpretation of Satellite Oceanographic data (AVISO 1996) are based on an algorithm suitable for non-frozen open oceans. Therefore, the accuracy of the observed lake heights over the ice surfaces in these lakes may be degraded compared with the accuracy over sea surface (for more details see the discussion in Section 5). The two lakes in east China, namely Hongze and Gaoyou lakes, are located in areas with large populations and farming activity. Here water consumption is heavy and water levels are regulated, so the changes in lake levels may not correspond to climate variation. In addition, the size of Ngangzi Lake is only 244 km^2, which is about the size of a footprint of the Topex Microwave Radiometer (TMR), so here the wet tropospheric delay of range cannot be accurately measured by the TMR; in fact, for some reason only one of these six lakes, namely Hulun Lake, contains TMR water vapour measurements (see the next section).

3 LAKE LEVELS FROM TOPEX/POSEIDON ALTIMETRY

3.1 Altimeter data processing

The T/P data we used are from AVISO (1996) and cover repeat T/P cycles 10 (1992 December 21) to 351 (2002 October 20), spanning about 10 yr. In a typical oceanographic application, only altimeter ranges over the oceans are retained when processing the GDRs to obtain corrected range measurements. However, to obtain inland lake levels it is necessary to retain data over land. Adopting the strategy used by Mercier *et al.* (2002), we applied dry tropospheric correction, ionosphere correction, sea-state bias, solid-earth tide, pole tide and instrument bias to the raw T/P-derived lake heights.

In the AVISO GDRs over China, except at Hulun Lake, neither an assimilated value nor the TMR value is available for the wet tropospheric correction. Therefore, we use the following formula to

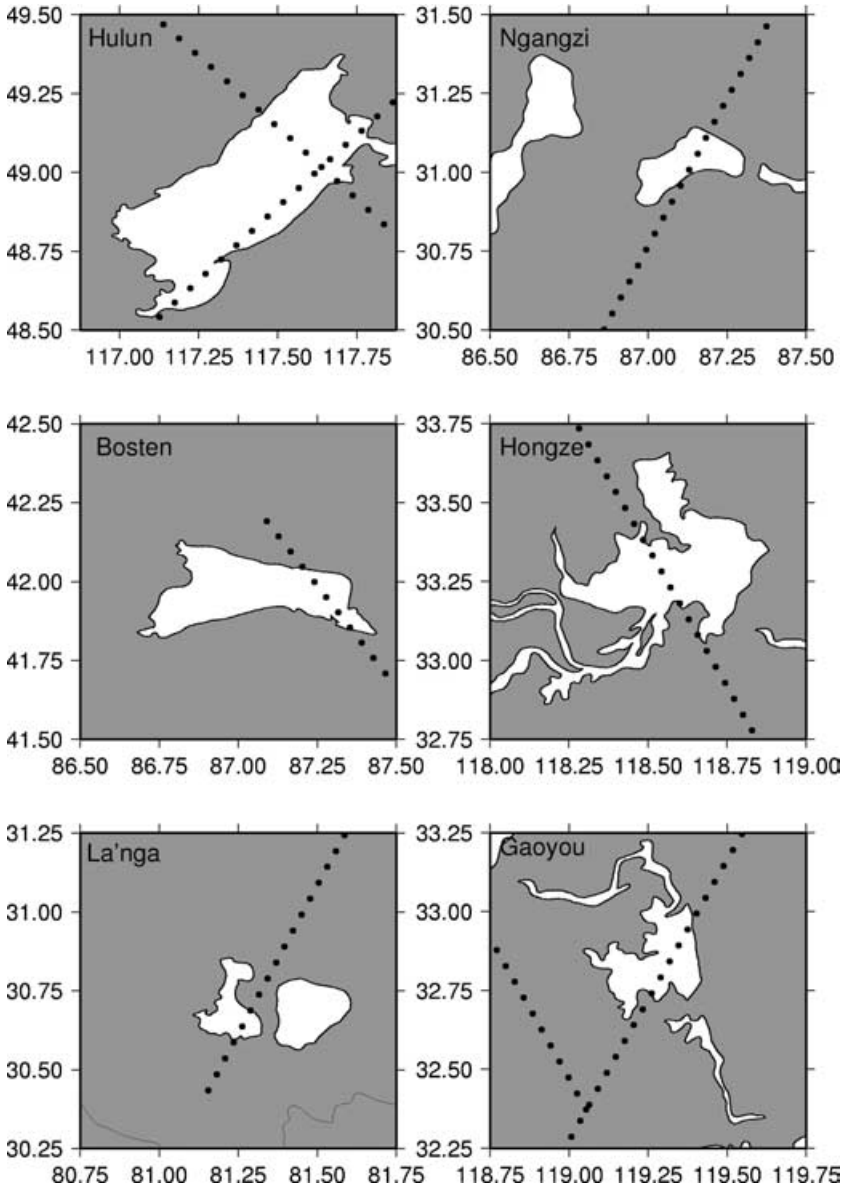

Figure 2. T/P ground tracks over the six studied lakes in China. Circles represent locations of 1-Hz T/P observations.

compute wet tropospheric corrections (Chelton *et al.* 2002):

$$\Delta R_{\rm vap} \approx \frac{\beta'_{\rm vap}}{T_{\rm eff}} \int_0^R \rho_{\rm vap}(z)\,dz \approx 6.19 \int_0^R \rho_{\rm vap}(z)\,dz, \quad (1)$$

where $\rho_{\rm vap}(z)$ is the water vapour density at height z, and R is the maximum height considered for the integration. The constant $\beta'_{\rm vap}/T_{\rm eff} = 6.19$ (cm^3 g^{-1}) is based on the approximate value $\beta'_{\rm vap} = 1720.6$ (°K cm^3 g^{-1}) and the effective temperature $T_{\rm eff} = 278$°K for the mid-latitude area (Chelton *et al.* 2002). Eq. (1) requires values of $\rho_{\rm vap}(z)$ up to R, which were obtained from the National Center for Environmental Prediction (NCEP) (see the web site http://wesley.ncep.noaa.gov).

The temporal and spatial resolutions of currently available assimilated water vapour by NCEP are six hours and 2.5° × 2.5°, respectively, which are quite coarse compared with the variability of atmospheric moisture, which is typically of the order of hours and several kilometres. To obtain reliable wet tropospheric corrections from the assimilated data, precise collocations in space and time for the T/P altimeter ranges are essential. The wet tropospheric correction ranges from a few centimetres to decimetres, and its variation is largely annual; that is, it is high in the summer and low in winter. Fig. 3 shows a comparison of wet tropospheric corrections from NCEP (this study, eq. 1), ECMWF (provided in the AVISO GDRs) and TMR measurements over Lake Huron in North America. Lake Huron is chosen because of its large size and the availability of TMR data. Over Lake Huron the NCEP and ECMWF results agree quite well, with the differences amounting to about 3 cm RMS. The NCEP and ECMWF results are also quite consistent with the TMR results, the differences again being about 3 cm RMS.

Because the lakes under study are relatively small in size compared with large lakes such as the Great Lakes in North America, all lakes, except Hulun Lake, contain only one T/P ground track. The arcs over these lakes are also very short, containing only a few 1-Hz data points. To avoid using bad altimetry data, affected by contaminated waveforms (Deng *et al.* 2002), any data point that is

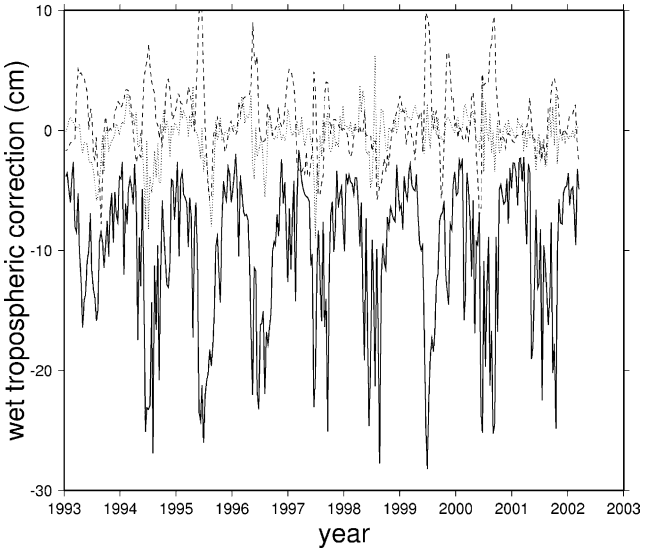

Figure 3. Comparison of water vapour corrections over Lake Huron in North America. The thick line is from TMR, the dotted line is the difference between ECMWF and TMR, and the dashed line is the difference between NCEP and TMR.

Table 2. Percentage of TOPEX/Poseidon cycles that yield useable data.

Lake	Hulun	Bosten	La'nga	Ngangzi	Hongze	Gaoyou
Percentage	71.92	41.52	36.84	43.86	54.68	61.12

10 km within the lakeshore is disregarded. The numbers of 1-Hz data points used for the six lakes are listed in Table 1. The worst cases are La'nga and Ngangzi lakes, with only one 1-Hz point available for each lake. As such, it is expected that the T/P-derived lake levels over China contain a high noise level, requiring filtering.

Since T/P does not repeat exactly the same ground track (off by at most 1 km), reductions of lake heights along individual repeat passes to a reference pass are necessary. To do this, we regard the geoid gradient computed from the EGM96 geopotential field (Lemoine *et al.* 1998) as the surface gradient of a given lake. The reduction of the lake height from an arbitrary pass to the reference pass is made using the relation

$$LL' = LL + (N - N'), \tag{2}$$

where LL and N are the lake height and geoid undulation at an arbitrary pass, and LL' and N' are their counterparts at the reference pass. The geoidal undulations in eq. (2) were computed from the EGM96 gravity model (Lemoine *et al.* 1998) up to degree 360. For each lake we selected as the reference pass that pass that contains the most data points. In most lakes under study, at a given reference point the T/P-measured lake height from one cycle can be significantly different from that from the next cycle, and in some cases the difference reaches several metres. In order to obtain robust estimates of lake heights, for each reference point the median of the lake heights from T/P cycles 10 to 351 was first computed. Any individual lake height that differs from the median by more than three times the standard deviation of the raw time series of lake height was disregarded. The cleaned lake heights were then used to compute the simple mean of the lake height at the reference point. The lake level anomaly (LLA) is obtained by subtracting the mean from the individual lake height. Table 2 shows the percentages of cycles that gave useable data.

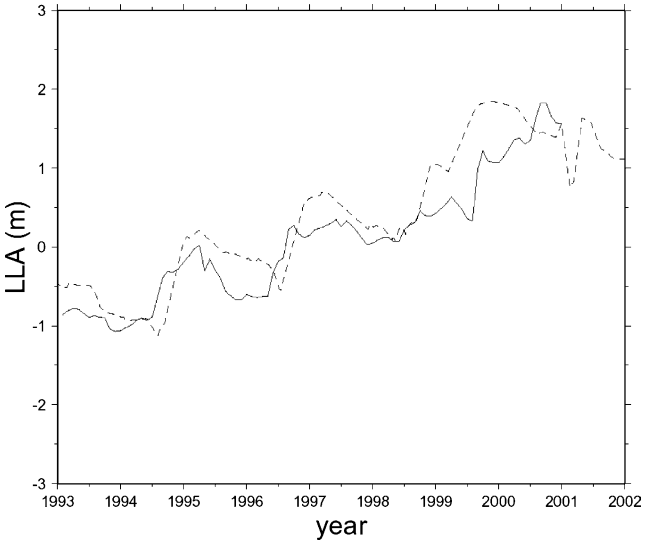

Figure 4. Comparison of T/P-derived (dashed line) and *in situ* (solid line) lake levels at Bosten Lake.

3.2 Verification

Despite considerable efforts to obtain *in situ* lake gauge records for the six lakes under study, only records at Bosten Lake were made available to the authors. Fig. 4 shows a comparison of monthly lake levels derived from T/P and from the lake gauge records collected by Wang *et al.* (2003). We also made an 'indirect' verification by comparing the T/P-derived lake levels (by the method listed in Section 3.1) and *in situ* gauge records for Lake Huron. As shown in Fig. 5, there are two T/P passes over Lake Huron, and Pass 152 was selected to compute the LLA from cycle 10 to cycle 351. The *in situ* records are from the Center for Operational Oceanographic Products and Services (CO-OPS) of the National Ocean and Atmosphere Administration (NOAA) (see also the web site http://www.co-ops.nos.noaa.gov/). Again, as shown in Fig. 5, the T/P-derived and *in situ* LLAs agree very well, with a RMS difference of 3.76 cm. This agreement is consistent with that obtained by Morris & Gill (1994), who used a shorter data record. The patterns of annual variation from T/P and *in situ* data are very coherent, and the decreasing trends of the Lake Huron level since 1998 from the two data sets are also very consistent. These comparisons at Hulun Lake and Lake Huron show that the T/P processing technique and geophysical corrections for the six lakes over China are adequate.

4 RESULTS

4.1 Lake-level time series and their wavelet spectra

We have computed time series of LLA over the six lakes, and the results are shown in Fig. 6. As expected, the time series in Fig. 6 are rather noisy. In the figure, both the original time series and the filtered time series are given. The filtering in Fig. 6 was done using a Gaussian filter with a window of one year: see Wessel & Smith (1995). The time series of lake levels in Fig. 6 show intraseasonal, seasonal and interannual variations. In order to identify the time-frequency characteristics of the lake levels, the lake-level time series were wavelet-transformed using

$$C(a, b) = \frac{1}{\sqrt{a}} \int_{-\infty}^{\infty} f(t)\psi\left(\frac{t-b}{a}\right) dt \tag{3}$$

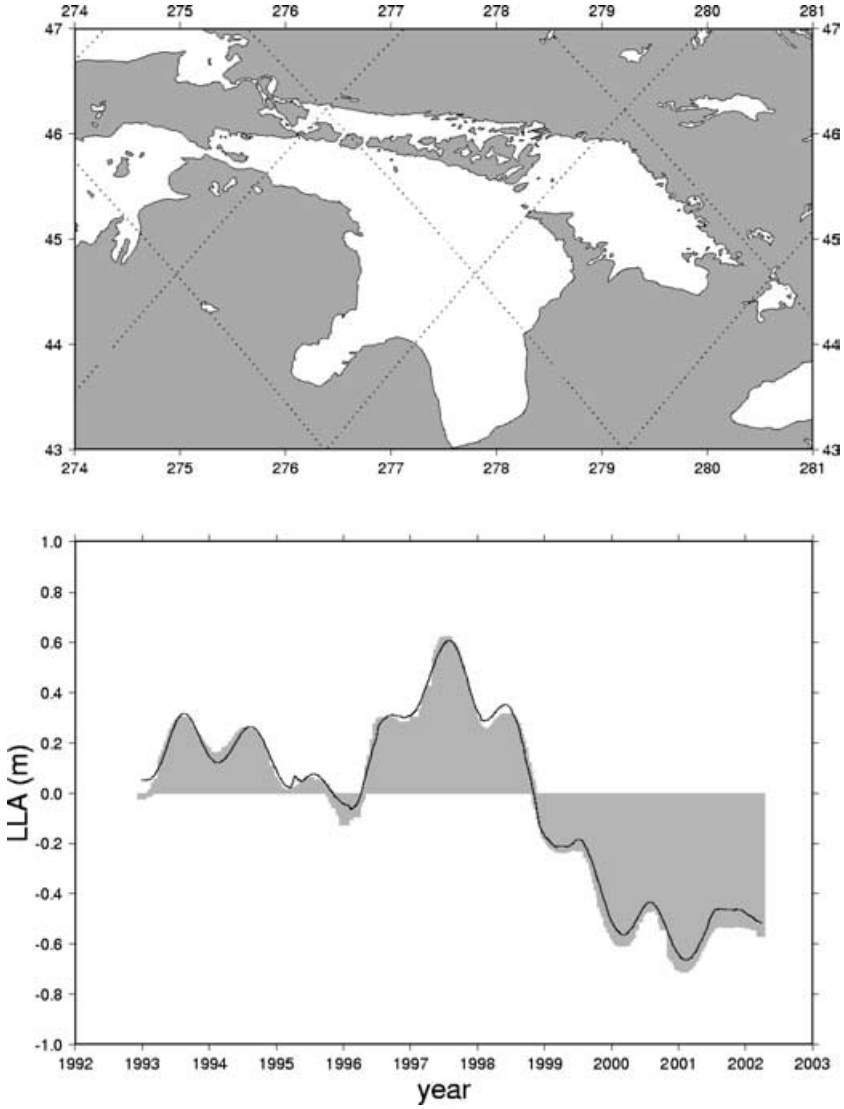

Figure 5. T/P ground tracks over Lake Huron and a comparison of T/P-derived (solid line) and *in situ* (shaded) lake levels.

(Daubechies 1992), where $f(t)$ is the lake level, a and b are scale and translation, respectively, ψ (t) is the wavelet function, and $C(a, b)$ is the wavelet coefficient. In this study, we choose ψ (t) to be the real part of the Morlet wavelet, defined as

$$\psi(t) = \pi^{-1/4} e^{-t^2/2} \cos(5t). \quad (4)$$

The Morlet wavelet (in complex or real form) is widely used in geophysical data analysis—see Kumar & Foufoula-Georgiou (1994) and Hwang & Chen (2000). The relationship between the scale a and its corresponding period p (or wavelength) in a conventional Fourier analysis for the Morlet wavelet in eq. (4) is $p = 1.232a$ (Torrence & Compo 1998).

Fig. 7 shows the wavelet coefficients of lake levels computed with the Morlet wavelet. The colour scale in Fig. 7 is such that the most negative scale and the most positive scale imply the maximum negative and the maximum positive time-wise correlations, respectively, between a frequency component and the Morlet wavelet at a given scale and translation (Hwang & Chen 2000). Zero value in the colour scale indicates the least time-wise correlation. For example, if one is looking for the seasonal cycle at a particular lake and its varying strength over the years, one should examine the colour scales at 12 month of the vertical coordinate, from 1993 to 2002. A purple or a blue scale implies the seasonal low and a red scale implies the seasonal high. A summary of the detected frequency components and their variations in the lake levels is given below.

(1) Hulun Lake

Semi-annual, annual and interannual components are found in the Hulun lake-level variation. The semi-annual components are weak in most years. In 1999 and 2000, the annual components are also weak. Seasonally, the lake level is low in winter (December to March) and high in summer (June to August). Interannually, lows are found in 1995–1996, 1997–1998 and 2001, while highs are found in 1996 and 2000. Therefore, as a rough estimate, the period of the interannual variation of Hulun lake level is about 2 to 3 yr.

(2) Bosten Lake

As for Hulun Lake, the variation in Bosten lake level also contains semi-annual, annual and interannual components. Again, the semi-annual components are mostly weak over 1993–2002. The amplitude of the annual component varies from year to year, and is largest over 1996–2002 and smallest before 1996. In general, the high of lake level occurs from January to March and the low occurs from June to

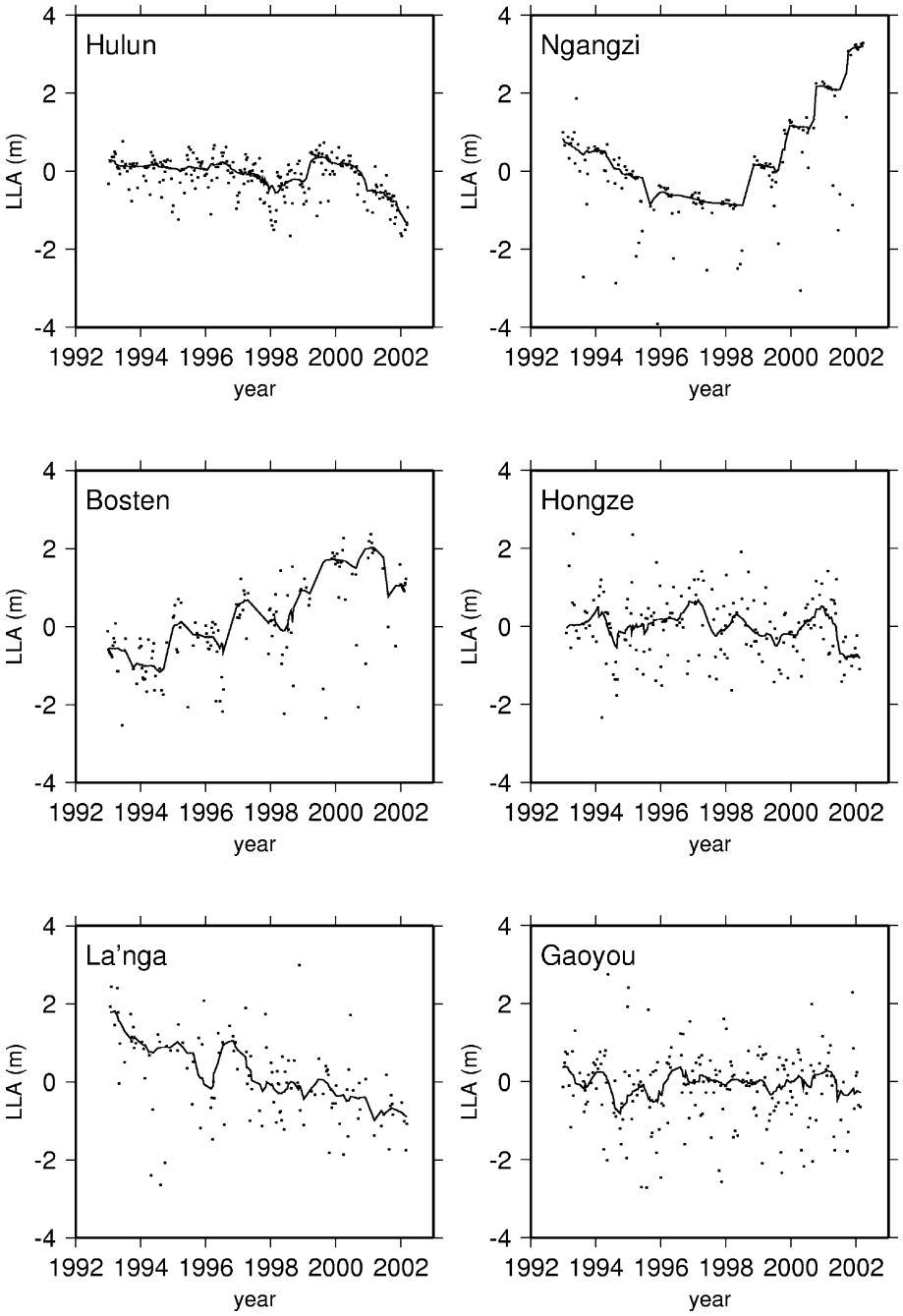

Figure 6. Lake-level anomalies (LLA) derived from T/P altimetry over the six lakes in China. Dots represent the raw LLA while the solid lines represent the filtered LLA.

October. The low lake level in summer is the result of the large water consumption (e.g. irrigation) in summer. There is a weak biennial oscillation in the lake level. At the interannual timescale, there is a weak peak in 1997–1998 (concurrent with the largest El Niño in the 1990s), and there are strong lows in 1993 and 1996, which are the La Niña years.

(3) La'nga Lake

The variation in La'nga lake level contains annual and interannual components. There is a weak semi-annual variation, but the pattern is irregular. Seasonally, lows of lake level occur in summer and highs occur in winter, but this pattern becomes irregular after 1998. This lake is closed and frozen in winter. Therefore, the lake level is high due to the increased volume of the lake in winter. Interannual oscillation exists, but there is no clear period.

(4) Ngangzi lake

There are evident annual and interannual variations in the lake level. The semi-annual variation is weak but evident, and is caused by the summer and winter monsoons. Annual variation is quite clearly evident, with lows in summer and highs in winter. After 1998, the amplitude of the annual component is enhanced. The reason for the annual low and high is the same as that for La'nga Lake. Again, as for La'nga Lake, there is no clear period in the interannual oscillation.

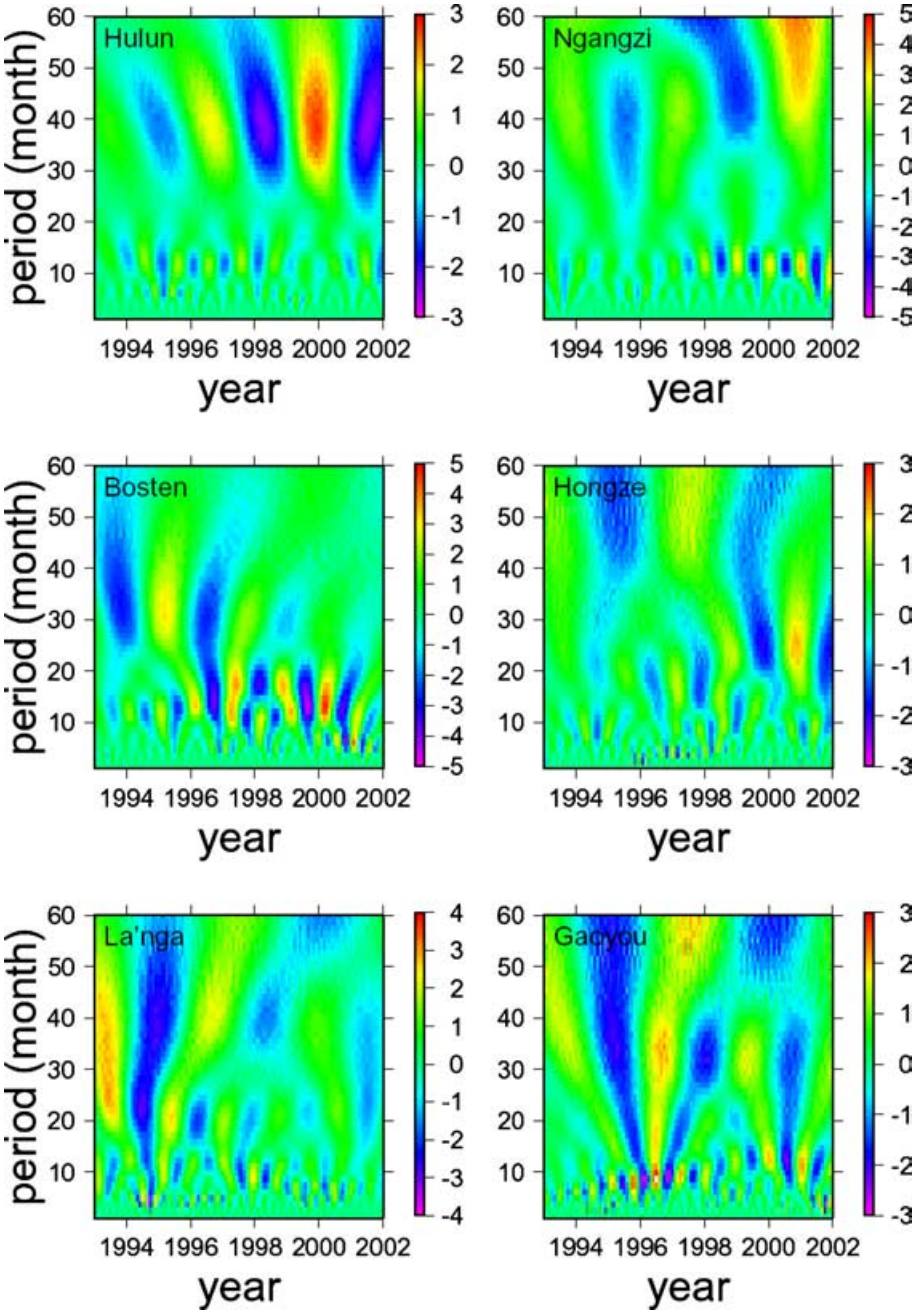

Figure 7. Wavelet spectra of LLA using the Morlet wavelets.

(5) Hongze and Gaoyou lakes

Owing to poor-quality data, no clear pattern of annual variation is seen in these two lakes. There is no clear period of interannual oscillation. However, the two lake levels contain semi-annual variations that are caused by winter and summer monsoons.

4.2 Trends and interannual variations of lake level associated with precipitation and ENSO

In order to see a possible connection of the lake levels over China with climate change, time series of the NINO3 sea-surface temperature anomaly (SSTA) and precipitation were obtained. The NINO3 SSTA is the area-averaged SSTA in the equatorial Pacific covering the area 5°S–5° N, 150°–90°W (http://rainbow.ldeo.columbia.edu/ees/data/). The NINO3 SSTA is widely used as an index of ENSO (Kiladis & Diaz 1989). The monthly precipitation time series were compiled at Beijing University as described by Wang *et al.* (2000) based on *in situ* observations for the period 1951 to 2001. Among the many rain stations used by Wang *et al.* (2000), only those at Hulun, Bosten and Ngangzi lakes were made available to the authors (see Fig. 1). Power spectral analysis by Wang *et al.* (2000) indicates that the precipitation in China is correlated to ENSO at the interannual timescale and also contains interdecadal variations. For comparison with lake level, the precipitation anomaly (PA) was computed by removing the climatological annual cycle (based on the 50-yr data) from the individual monthly

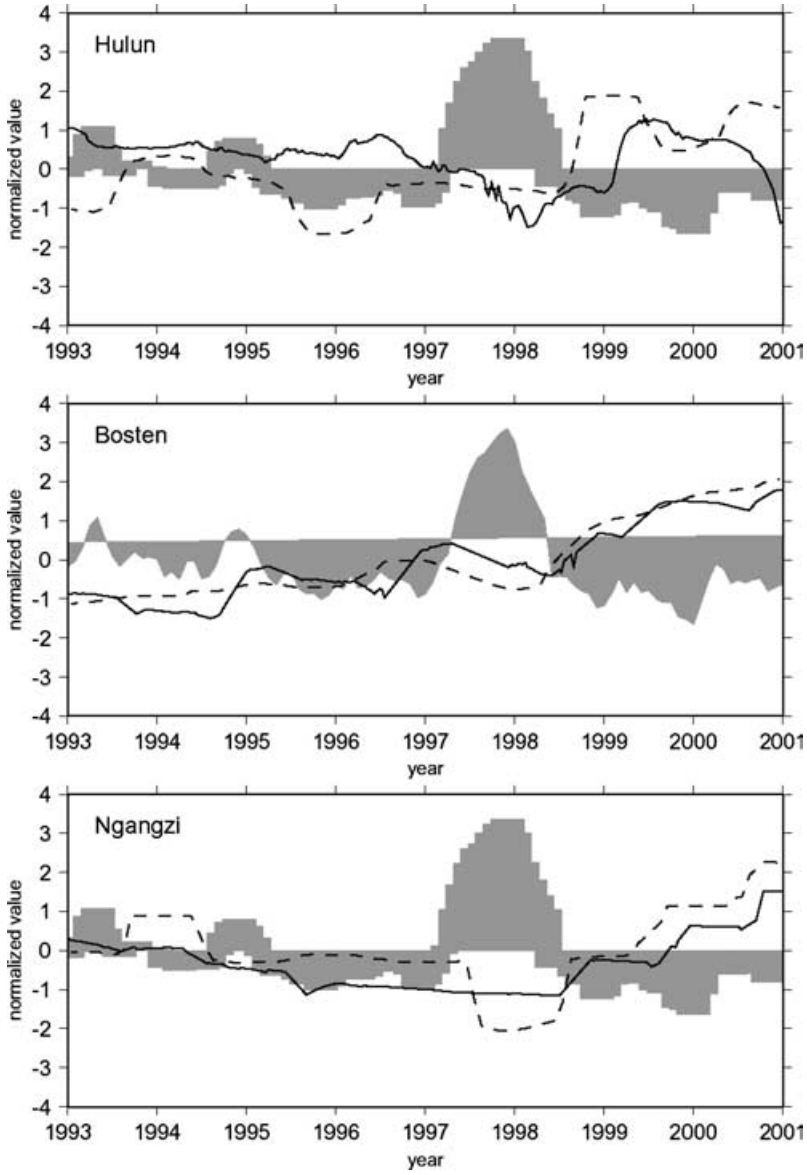

Figure 8. Comparison of normalized lake-level anomalies (solid line), precipitation anomalies (dashed line), and NINO3 sea-surface temperature anomalies (shaded) at Hulun, Bosten and Ngangzi lakes.

precipitations, and then the cumulative precipitation anomaly (CPA) computed. By assuming that the climatological annual precipitation cycle is in equilibrium with climatological values of transevaporation and other losses averaged in the catchment area enclosing the respective lake, the CPA is compared with the anomalous lake level in this study.

Fig. 8 shows the normalized values of LLA, NINO3 SSTA and CPA at Hulun, Bosten and Ngangzi lakes. A normalized value, x', of the original value, x, is computed by $x' = (x - \bar{x})/\sigma$, where $\bar{x}$ and σ are the mean and the standard deviation of the given time series. As seen in Fig. 8, for the period 1992–2001, a weak warming in the eastern Pacific (positive NINO3) appeared in 1992–1993 and 1994–1995, and a major warming appeared in 1997–1998. Following each of the warm events, cold events (La Niña) were evident. The cold event tends to last longer than the warm event, as seen in 1996 and 1999–2001. From Fig. 8, at Hulun, Bosten and Ngangzi lakes the slopes of LLA and CPA over the period 1993 January – 1997 December are distinctly different from those over 1998 January – 2001 December. Table 3 lists the slopes of LLA and CPA over these two periods. The 1997–1998 El Niño is a major climate event which impacts a number of phenomena. For example, the sign of the slope of the Earth's J_2 gravity coefficient changes from negative to positive after the 1997–1998 El Niño (Cox & Chao 2002).

Below is a discussion of all LLAs regarding the trends and interannual variations associated with ENSO. Possible links of LLA to precipitation at Hulun, Bosten and Ngangzi lakes also discussed.

(1) Hulun Lake

In general, the Hulun lake level decreased steadily before 1997 December, in accordance with the decreasing precipitation. The correlation between LLA and CPA is low here (<0.2), although some common trends over certain periods can be found. Huang *et al.* (2000) and Shi *et al.* (2002) showed that, in the developing stage of the 199–1998 El Nino (from 1997 May to 1997

Table 3. Slopes of lake level and precipitation over two different periods at three lakes.

Lake	Slope of lake level (cm yr^{-1}) 1/1993–12/1997, 1/1998–12/2001	Slope of precipitation (mm yr^{-1}) 1/1993–12/1997, 1/1998–12/2001
Hulun	−6.7, −8.9	−4.5, 34.2
Bosten	26,7, 72.3	24.5, 130.1
Ngangzi	−37.3, 100.3	−23.6, 101.8

November), drought occurred in north China, while in the decaying stage (from 1998 May onwards), floods occurred in north China and the Yangtze River. This description fits the trends of LLA and CPA over the period 1997 May – 1999 August. Specifically, in 1997 the Hulun lake level dropped continuously until it reached its lowest level in 1998 January, which was coincident with the peak of the 1997–1998 El Niño (1997 December). From 1998 May to 1999 September, the lake level rose steadily. However, from 1999 September onwards, the lake level again decreased, which is consistent with the decreasing trend of precipitation. (Note that the peak of CPA leads that of LLA by 3–4 months.) During the 1996 La Niña, the precipitation dropped abnormally, while the lake level was not affected.

(2) Bosten Lake

The Bosten lake level increased steadily from 1993 to 2001 by more than 2 m. The correlation coefficient between the LLA and CPA at Bosten Lake is 0.78. The rising trend of the Bosten lake level is fully consistent with the result reported by Wang *et al.* (2003). According to Wang *et al.* (2003), the increase of the Bosten lake level was caused by the increased melting snow on Tianshan Mountain, which is the major water catchment area for Bosten Lake. The driving factor for the increased snow is temperature, as records show a steady rise in temperature over this region (Wang *et al.* 2003). While the CPA rose almost monotonically (except for a drop in 1997 December), the LLA fluctuates; in particular, there are LLA lows in the summers of 1994, 1996 and 1998. Of special note are the low of CPA in 1997 December and a low of LLA in 1998 August, which occurred during the 1997–1998 El Niño. Since these lows, the rising trends of temperature and lake level are large in comparison with the rising trends before 1998.

(3) La'nga and Ngangzi lakes

These two lakes are located in Tibet. From 1993 to 2002, the La'nga lake level dropped by about 3 m (the slope is −27.2 cm yr^{-1}). The drop in the La'nga lake level had natural and man-made causes. The natural cause is obviously drought (see the precipitation time series near Ngangzi Lake), and the man-made cause could be the heavy water consumption (La'nga Lake is a famous tourist attraction in Tibet). There is a sharp drop in the LLA at La'nga Lake in the summer of 1996, followed by a rapid rise, which persists until 1996 December, and then the trend reverses. The La'nga Lake level experienced no anomalous change during the 1997–1998 El Niño. Like the La'nga lake level, the Ngangzi lake level dropped by about 2 m from 1993 to 1998. However, unlike the La'nga lake level, the Ngangzi lake level trend reversed in 1997 December and the lake level increased steadily by about 4 m from 1998 to 2001. The precipitation slope also reversed from negative to positive in 1998. The correlation coefficient between the LLA and CPA at Ngangzi Lake is 0.50, which is significant. In 1997 December, the precipitation and the lake level over Ngangzi Lake hit their lowest values, and the lake level has increased steadily since then. One interesting difference is that, while the La'nga lake level continued to drop after 1998 January, the Ngangzi lake level has increased steadily since 1998 January. This difference can be explained by the climate pattern in Tibet. The moisture in Tibet largely comes from the Indian Ocean through the river valleys in southeastern Tibet. The moisture rarely reaches western Tibet, and the general climate pattern is that western Tibet is dry while eastern Tibet is wet. Such a climate pattern is also revealed by satellite data (Ueno 1998). La'nga Lake is located 550 km west of Ngangzi Lake, so it receives less moisture than Ngangzi Lake. Furthermore, Ngangzi Lake is located in east Tibet, so it will be more sensitive to climate change in the Indian Ocean than La'nga Lake. This is why the lake-level slope of Ngangzi changes rapidly after 1998, while the slope of La'nga remains unchanged. A recent study by Thompson *et al.* (2000) using ice cores retrieved from southern Tibet (at 28 28°2 3′N and 85°4 3′E) shows that the climate of Tibet is sensitive to the fluctuation of the South Asia monsoon, which is affected by ENSO. Liu & Chen's (2000) study indicates that the Tibetan Plateau has experienced a significant warming in the past decade (1990–2000) and pointed out the Tibetan Plateau is one of the most sensitive areas to respond to global climate change.

(4) Hongze and Gaoyou Lakes

These two lakes are close to each other and are located in heavily populated areas. Both lake levels decreased slightly over 1993–2002, and the slopes of lake levels of Hongze and Gaoyou Lakes are −7.2 and −5.4 cm yr^{-1}, respectively. Over these two lakes human activity is abundant and there are man-made objects on the lakes, so the data quality here is degraded due primarily to contaminated returned radar waveforms. Therefore, the interannual fluctuations seen in Figs 5 and 6 are probably due to data noise and are not very reliable.

5 DISCUSSION: CONTAMINATED WAVEFORMS OVER LAKES IN CHINA

The results so far have shown that the T/P GDRs, which were created originally for oceanic applications, yield meaningful lake levels and associated climate signals over six lakes in China. However, our analysis also indicates that the T/P-derived lake-level series over China are relatively degraded in quality compared with what was obtained at large lakes such as Lake Huron in North America: see Fig. 5 and the result in Morris & Gill (1994). Poor geophysical corrections have been in part responsible for this degraded quality. A contributory factor is contaminated waveforms over the lakes in China. As an example, Fig. 9 shows the TOPEX waveforms over Lake Huron and Bosten Lake sampled at 10 Hz: the waveforms are significantly different. Bosten Lake is small in size compared with Lake Huron, and the depth of the former (8.15 m on average) is shallower than that of the latter. Small size and shallow depth combine to yield contaminated waveforms: small size allows a radar pulse to descend on both land and water surfaces, and shallow depth allows the penetrating pulse to hit the lake bottom and then to create a secondary return power (Zwally & Brenner 2002). A small lake tends to have a calm water surface that will yield a very narrow trailing edge

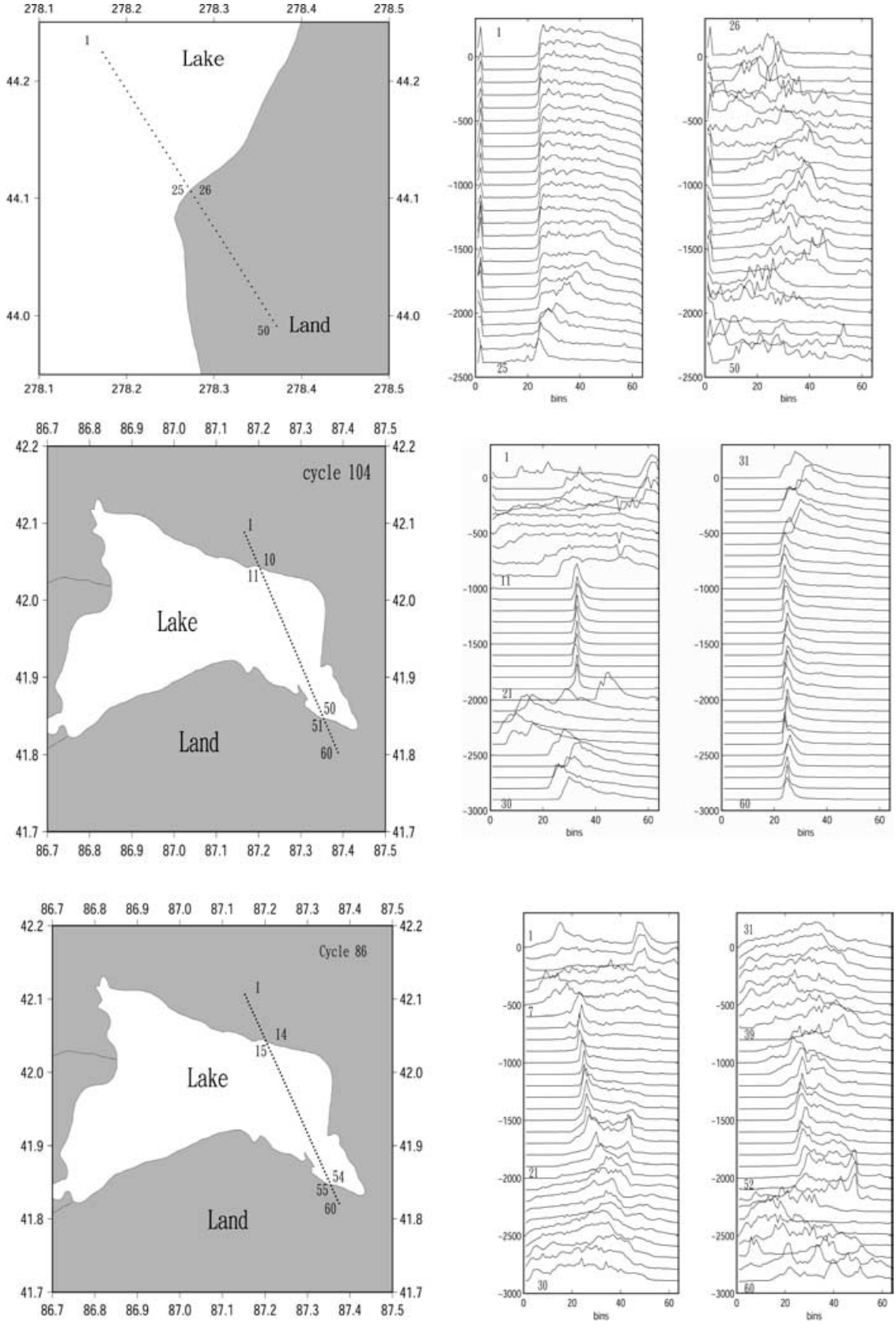

Figure 9. Waveforms from TOPEX sampled at 10 Hz over Lake Huron (top) and Bosten Lake in winter (middle, 1995 January) and in summer (bottom, 1995 July). The left panel shows the ground tracks, and the right panel shows the return power with respect to bin (or time). Each waveform series is offset by a constant. The inserted numbers show the sequence of 10-Hz waveforms since the first point.

in the return waveforms, which are also contaminated. These contaminated waveforms cannot be accurately tracked by the onboard tracker, which is optimized for ocean waveforms, and so cannot yield correct ranges between the satellite and the nadir surface. As shown in Fig. 9, the waveforms over Lake Huron have sharp leading edges and wide trailing edges that closely resemble the waveforms over the open, deep oceans. The waveforms over Bosten Lake have narrow trailing edges such as typically occur over ice surfaces and calm water surfaces. At the centre of Bosten Lake, where the lake depth approaches zero due to heavy sedimentation, the waveforms are very irregular and similar to those over land. These seriously contaminated waveforms will also occur over Hongze and Gaoyou lakes, where the averaged depths are less than 2 m. La'ngra and Ngangzi lakes are relatively deep (over 100 m), but their sizes are small so waveform contamination will still occur. The best conditions for determining lake level are for Hulun Lake because it has a relatively large size and contains a relatively long T/P arc. The waveform contamination can be miti by retracking the waveforms using specially designed retrackers; see, for example, Berry (2000) and Deng *et al.* (2002). Retracked waveforms will yield an improved accuracy of lake heights.

6 CONCLUSIONS

About 10 yr of T/P data were processed to obtain time series of lake levels at six inland lakes in China, and the T/P-derived lake level over Bosten Lake is validated by *in situ* data. Wavelet spectra of these lake-level time series show oscillations at different timescales. These lake levels are mostly affected by climate change. In particular, the lake levels of Hulun, Bosten and Ngangzi are correlated with precipitation and they all responded to the 1997–1998 El Niño. One interesting phenomenon is that the slope of the Ngangzi lake level changes from negative to positive after the 1997–1998 El Niño; the cause is left to climate modellers. The T/P follow-on mission, Jason-1, will continue to provide time series of lake level for these lakes, and it will be possible to see the interdecadal lake-level changes. There are no T/P and Jason-1 passes over some of the lakes on the Tibetan Plateau and the largest lake in China, Qinghai Lake, but here altimetry data from other missions such as ERS-1 and Envisat may be available. The problem of contaminated waveforms is discussed in relation to the size and depth of the six lakes. We expect that retracking of T/P waveforms could improve the accuracy of altimeter range measurements over the inland lakes of China, and retracking results will be presented in a future work.

ACKNOWLEDGMENTS

We thank J. Zhu for providing the rainfall data and AVISO for providing the T/P altimetry data. The gauge records of Bosten Lake were made available by R. Wang. We thank A. Bingham of JPL for providing the TOPEX waveforms, and X.-J. Dong for retrieving the waveforms.

REFERENCES

Alsdorf, D., Birkett, C., Dunne, T., Melack, J. & Hess, L., 2001. Water level changes in a large Amazon lake measured with spaceborne radar interferometry and altimetry, *Geophys. Res. Lett.,* **28,** 2671–2674.

Archivings Validation and Interpretation of Satellite Oceanographic data (AVISO), 1996. *AVISO User Handbook for Merged TOPEX/Poseidon Products,* 3rd edn.

Berry, P., 2000. Topography from land radar altimeter data: possibilities and restrictions, *Phys. Chem. Earth,* **25,** 81–88.

Berry, P., 2003. Global land scale hydrology monitoring using satellite altimetry, in *Proc. Int. Un. Geod. Geophys.,* .

Birkett, C.M., 1995. The contribution of TOPEX/POSEIDON to the global monitoring of climatically sensitive lakes, *J. geophys. Res.,* **100,** 25 179–25 204.

Chelton, D.B., Ries, J., Haines, B.J., Fu, L.L. & Callahan, P.S., 2002. Satellite altimetry, in, *Satellite Altimetry and Earth Sciences, a Handbook of Techniques and Applications,* pp. 1–131, eds Fu, L.L. & Cazenave, A., Academic Press, New York.

Cox, C.M. & Chao, B.F., 2002. Detection of a large scale mass redistribution in the terrestrial system since 1998, *Science,* **297,** 831–833.

Daubechies, I., 1992. *Ten Lectures on Wavelets,* Soc. for Ind. and Appl. Math., Philadelphia.

Deng, X., Featherstone, W.E., Hwang, C. & Berry, P.A.M., 2002. Estimation of contamination of ERS-2 and POSEIDON satellite radar altimetry close to the coasts of Australia, *Mar. Geod.,* **25,** 249–271.

Fu, L.-L., Edward, E.J., Christensen, J., Yamarone, C.A. Jr, Lefebvre, M., Ménard, Y., Dorrer, M. & Escudier, P., 1994. TOPEX/POSEIDON mission overview, *J. geophys. Res.,* **24,** 24 369–24 381.

Huang, R.H., Zhang, R.H. & Zhang, Q.Y., 2000. The 1997/98 ENSO cycle and its impact on summer climate anomalies in East Asia, *Adv. atm. Sci.,* **17,** 348–362.

Hwang, C. & Chen, S.-A., 2000. Fourier and wavelet analyses of TOPEX/POSEIDON-derived sea level anomalies over the South China Sea: a contribution to SCSMEX, *J. geophys. Res.,* **105,** 28 785–28 804.

Kiladis, G.N. & Diaz, H.F., 1989. Global climatic anomalies associated with extremes in the Southern Oscillation, *J. Clim.,* **2,** 1069–1090.

Kumar, P. & Foufoula-Georgiou, E., 1994. Wavelet Analysis in Geophysics: An Introduction, *Wavelets in Geophysics,* eds Foufoula-Georgiou, E. & Kumar, P., pp. 1–44, Academic Press, San Diego.

Lemoine, F.G. *et al.*, 1998. The Development of Joint NASA GSFC and the National Imagery and Mapping Agency (NIMA) Geopotential Model EGM96, *Rep. No. NASA/TP–206861*, National Aeronautics and Space Administration, Greenbelt, MD.

Liu, X.D. & Chen, B.D., 2000. Climatic warming in the Tibetan Plateau during recent decades, *Int. J. Clim.,* **20,** 1729–1742.

Mercier, F., Cazenave, A. & Maheu, C., 2002. Interannual lake level fluctuations (1993–1999) in Africa from Topex/Poseidon: connections with ocean-atmosphere interactions over the Indian Ocean, *Global Planet. Change,* **32,** 141–163.

Morris, C.S. & Gill, S.K., 1994. Evaluation of the TOPEX/POSEIDON altimeter system over the Great Lakes, *J. geophys. Res.,* **99,** 24 527–24 539.

Shi, N., Chen, L.W., Xia, D.D., 2002. A preliminary study on the global land annual precipitation associated with ENSO during 1948–2000, *Adv. Atm. Sci.,* **19,** 993–1003.

Thompson, L.G., Yao, T., Mosley-Thompson, E., Davis, M.E., Henderson, K.A. & Lin, P.-N., 2000. A high-resolution millennial record of the south Asian monsoon from Himalayan ice cores, *Science,* **289,** 1916–1919.

Torrence, C. & Compo, G., 1998. A practical guide to wavelet analysis, *Bull. Am. meteorol. Soc.,* **79,** 61–78.

Ueno, K., 1998. Characteristics of plateau-scale precipitation in Tibet estimated by satellite data during 1993 Monsoon season, *J. meteor. Soc. Japan,* **76,** 553–548.

Wang, S.W., Gong, D.Y., Ye, J.L. & Chen, Z.H., 2000. Seasonal precipitation series of eastern China since 1880 and variability, *Acta Geograph. Sinica,* **55,** 281–193.

Wang, R., Giese, E. & Gao, Q.Z., 2003. The recent change of water level in the Bosten Lake and analysis of its causes, *J. Glaciol. Geocryology,* **25,** 60–64 (in Chinese).

Wessel, P. & Smith, W.H.F., 1995. New version of the Generic Mapping Tool released, *EOS, Trans. Am. geophys. Un.,* **76,** 329.

Zwally, H.J. & Brenner, A.C., 2002. Ice Sheet dyamics and mass balance, in *Satellite Altimetry and Earth Sciences, a Handbook of Techniques and Applications,* pp. 351–369, eds Fu, L.L. & Cazenave, A., Academic Press, New York.